TMX5/TXNDC15, a natural trapping mutant of the PDI family is a client of the proteostatic factor ERp44

Tatiana Soldà[1+], Carmela Galli[1+], Concetta Guerra[1], Carolin Hoefner[1, 2], Maurizio Molinari[1, 3*]

[1]Università della Svizzera italiana, Institute for Research in Biomedicine; CH-6500 Bellinzona, Switzerland
[2]Department of Biology, Swiss Federal Institute of Technology; CH-8093 Zurich, Switzerland
[3]School of Life Sciences, École Polytechnique Fédérale de Lausanne; CH-1015 Lausanne, Switzerland

*Corresponding author Email: maurizio.molinari@irb.usi.ch
+Equal contribution

The endoplasmic reticulum (ER) is the organelle of nucleated cells that produces lipids, sugars and proteins. More than 20 ER-resident members of the Protein Disulfide Isomerase (PDI) family regulate formation, isomerization and disassembly of covalent bonds in newly synthesized polypeptides. The PDI family includes few membrane-bound members. Among these, TMX1, TMX2, TMX3, TMX4 and TMX5 belong to the thioredoxin-related transmembrane (TMX) protein family. TMX5 is the least known member of the family. Here, we establish that TMX5 covalently engages via its active site cysteine residue at position 220 a subset of secretory proteins, mainly single- and multi-pass Golgi-resident polypeptides. TMX5 also interacts non-covalently, and covalently, via non-catalytic cysteine residues, with the PDI family members PDI, ERp57 and ERp44. The association of TMX5 and ERp44 requires formation of a mixed disulfide between the catalytic cysteine residue 29 of ERp44 and the non-catalytic cysteine residues 114 and/or 124 of TMX5 and controls the ER retention of TMX5. Thus, TMX5 belongs to the family of proteins including Ero1α, Ero1β, Prx4, ERAP1, SUMF1 that do not display ER retention sequences and rely on ERp44 engagement for proper inter-compartmental distribution.

Keywords

Endoplasmic reticulum; ERp44; ERp57; Oxidoreductase; PDI; Protein folding and quality control; TMX5.

Introduction

The protein disulfide isomerase superfamily includes more than 20 ER-resident members that ensure oxidative folding of newly synthesized polypeptides and participate in clearance of misfolded proteins from the ER lumen (Okumura *et al*, 2015; Patel *et al*, 2020; Pisoni & Molinari, 2016). Few of them, TMX1, TMX2, TMX3, TMX4 and TMX5 are anchored at the ER membrane (Guerra & Molinari, 2020). TMX1 (TXNDC1) is a reductase associated with mitochondria-ER contact sites. It regulates calcium flux and is involved in biogenesis and clearance of membrane-associated polypeptides (Guerra *et al*, 2018; Herrera-Cruz *et al*, 2021; Lynes *et al*, 2012; Matsuo *et al*, 2001; Matsuo *et al*, 2009; Pisoni *et al*, 2015; Raturi *et al*, 2016). TMX2 (TXNDC14) has the active site unconventionally located at the cytoplasmic site of the ER membrane. TMX2 regulates sulfenylation of mitochondrial proteins at mitochondria-ER contact sites to control calcium flux. It also localizes to the nuclear envelope, where it supports nuclear import of select cargo proteins (Chen *et al*, 2024; Guerra & Molinari, 2020; Lynes *et al.*, 2012; Oguro & Imaoka, 2019; Quimby & Corbett, 2001). TMX3 (TXNDC10) has a canonical CGHC active site sequence, which corresponds to the catalytic site of PDI. It has oxidase activity in vitro and its b' domain engages the oxidoreductase' clients. However, its biological role has not been established (Guerra & Molinari, 2020; Haugstetter *et al*, 2005; Haugstetter *et al*, 2007). TMX4 (TXNDC13) is a reductase located in the ER and in the nuclear envelope, where it regulates the disassembly of disulfide-bonded LINC complexes to promote selective clearance of excess outer nuclear membrane portions during recovery from ER stress (Guerra & Molinari, 2020; Hatahet & Ruddock, 2009; Kucinska *et al*, 2023; Kucinska & Molinari, 2024; Sugiura *et al*, 2010).

TMX5 (TXNDC15) is the least known member of the TMX family. It is a single-span type I protein of 360 amino acids with a large, penta-glycosylated luminal domain and a short C-terminal cytoplasmic tail lacking canonical ER retention signals. TMX5 has 5 cysteine residues (C in single letter code, green, **Fig. 1**). The cysteine at position 220 (red, **Fig. 1**) is embedded in a non-canonical CRFS active site that defines TMX5 as a natural trapping mutant protein (Yang *et al*, 2016). So far, no biological role has been ascribed to TMX5 but mutations in the *TMX5* gene have been associated with the development of the Meckel-Gruber syndrome (MKS), a rare perinatally lethal autosomal recessive disease caused by defective ciliogenesis (Deng & Xie, 2024; Hartill *et al*, 2017; Xu *et al*, 2024).

Here, we identify the endogenous client proteins trapped in mixed disulfides with the active site cysteine residue 220 of TMX5. We report that endogenous ERp57, PDI and ERp44 associate covalently with non-catalytic TMX5 cysteine residues. We characterize the association between TMX5 and the proteostatic factor ERp44 that controls the ER-to-Golgi cycling of proteins lacking ER retention motifs (Anelli *et al*, 2002). The association involves the TMX5's cysteine residues 114 and 124 and the ERp44 active site cysteine residue 29 and contributes to the ER retention of TMX5.

```
  1   MVPAAGRRPPRVMRLLGWWQVLLWVLGLPVRGVEVAEESGRLWSEEQPAH  50
 51   PLQVGAVYLGEEELLHDPMGQDRAAEEANAVLGLDTQGDHMVMLSVIPGE  100
                  114              124
101   AEDKVSSEPSGVTCGAGGAEDSRCNVRESLFSLDGAGAHFPDREEEYYTE  150
                            177
151   PEVAESDAAPTEDSNNTESLKSPKVNCEERNITGLENFTLKILNMSQDLM  200
                210       220
201   DFLNPNGSDCTLVLFYTPWCRFSASLAPHFNSLPRAFPALHFLALDASQH  250
251   SSLSTRFGTVAVPNILLFQGAKPMARFNHTDRTLETLKIFIFNQTGIEAK  300
301   KNVVVTQADQIGPLPSTLIKSVDWLLVFSLFFLISFIMYATIRTESIRWL  350
351   IPGQEQEHVE
```

C cysteine residues
C active site cysteine
N-glycosylation sites

Figure 1. TMX5/TXNDC15 features. TMX5 is a type I glycoprotein (the transmembrane domain is underlined). The CRFS unconventional active site and the active site cysteine residue at position 220 are shown in red. Asparagine residues (N in single letter code, in N-X-S/T consensus sequences for N-glycosylation) are shown in blue. The other 4 cysteine residues at position C114, C124, C177 and C210, whose role is established in this study are shown in green.

Results and Discussion

TMX5 localizes in the ER and the Golgi compartments

The presence of 5 N-linked glycans offers the possibility to establish if TMX5 is retained in the ER or traffics to the Golgi compartment by an EndoglycanaseH (EndoH)-sensitivity assay. In fact, upon arrival in the Golgi compartment, resident glycosyl transferases modify the glycoprotein's N-glycans resulting in an increase of the polypeptide's apparent molecular weight. Moreover, the N-glycans of proteins retained in the ER are cleaved off by EndoH, whereas the complex glycans generated in the Golgi compartment become resistant to EndoH cleavage (Rothman *et al*, 1984). TMX5 shows a heterogeneous electrophoretic mobility (green line, **Fig. 2A**). This is a symptom of complex glycosylation of TMX5 and indicates that a fraction of the polypeptide is transported to the Golgi compartment. To confirm this, we exposed the immunoisolated TMX5 to EndoH (Rothman *et al.*, 1984). These analyses reveal that about 20% of TMX5 displays EndoH-resistant oligosaccharides, thus it reaches the Golgi complex (**Fig. 2B**, lanes 1, 2). In addition to the active site Cys_{220}, TMX5 has 4 other cysteine residues at position 114, 124, 177, and 210 (**Figs. 1, 2C**). Individual mutations of Cys_{220}, Cys_{114}, or Cys_{124} do not affect the cycling of TMX5 between ER and Golgi as shown by the unchanged fraction of complex N-glycans displayed by the proteins (**Fig. 2B**, lanes 3-8). However, mutation of Cys_{177} (lanes 9, 10), or of Cys_{210} (lanes 11, 12), whose proximity in the TMX5 structure hints at their involvement in an intramolecular disulfide bond important to stabilize the TMX5 native structure (**Fig. 2C**), results in efficient retention of the protein in the ER (**Fig. 2B**, lanes 10 and 12). Consistent with the results of the EndoH assay (**Fig. 2B**), the analyses by confocal laser scanning microscopy (CLSM) of the subcellular localization of TMX5 and of the 5 cysteine mutants (**Figs. 2D-2I**) show that TMX5 (**Fig. 2D**), TMX5$_{C220A}$ (**Fig. 2E**), TMX5$_{C114A}$ (**Fig. 2F**), TMX5$_{C124A}$ (**Fig. 2G**) extensively co-localize with the ER marker CNX and with the Golgi marker Giantin. TMX5$_{C177A}$ (**Fig. 2H**) and TMX5$_{C210A}$ (**Fig. 2I**) are retained in the ER, possibly as a consequence of misfolding upon elimination of the structural intramolecular disulfide linking these two cysteine residues.

4
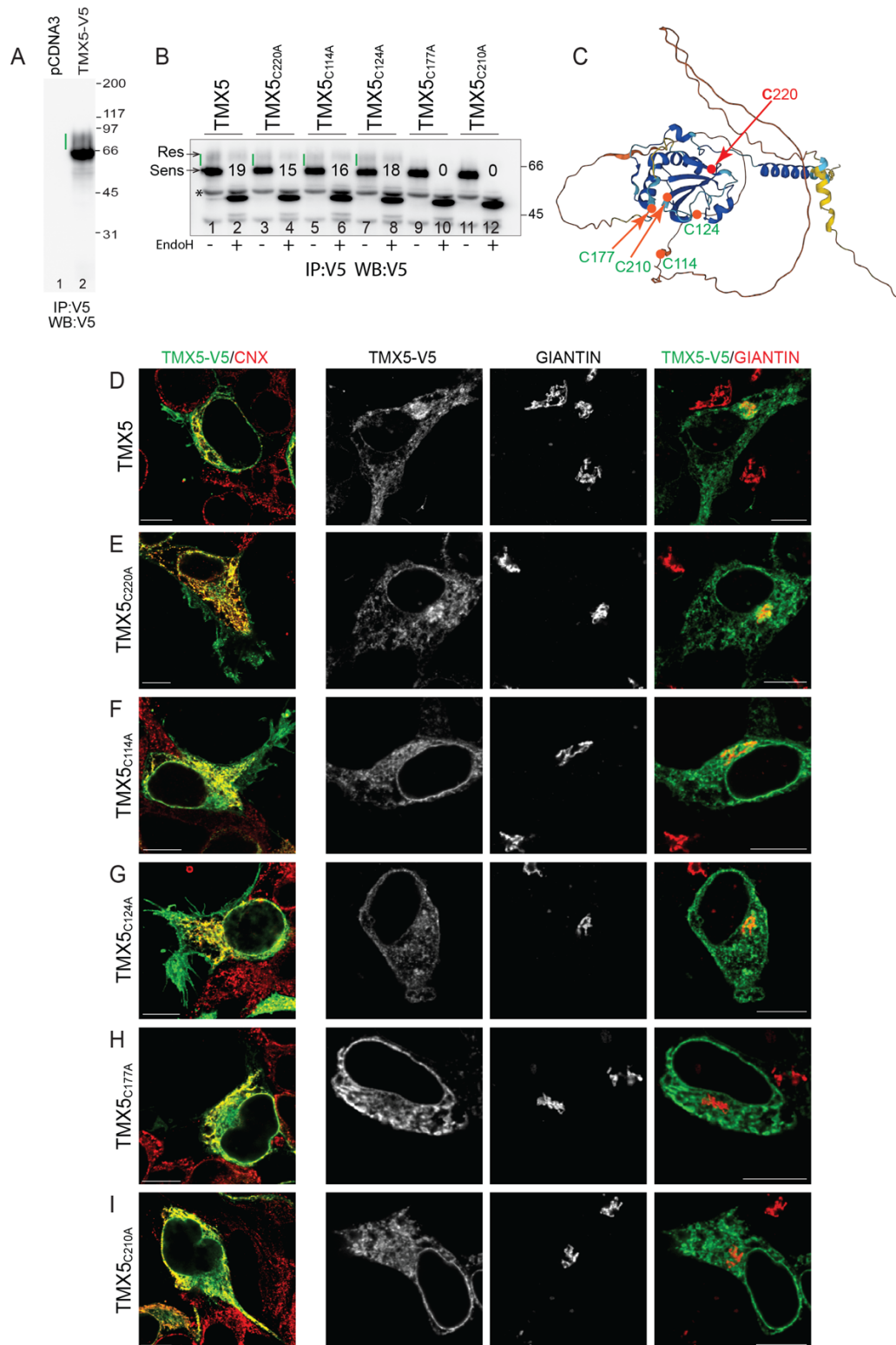
Figure 2. TMX5 localizes in the ER and Golgi. A TMX5 separated in a reducing gel (lane 2). The green line shows the complex glycosylated fraction of TMX5 (see panel **B**). **B** Assessment of EndoH-resistant N-glycans of TMX5 and TMX5 cysteine mutants. The % of EndoH-resistant TMX5's form is given for this experiment. **C** Predicted structure of TMX5, cysteine residues in green, active site cysteine 220 in red. The proximity of cysteine residues 177 and 210 in the TMX5 structure hint at their engagement in an intra-molecular disulfide bond (https://alphafold.ebi.ac.uk/entry/Q96J42). **D** Co-localization in IF of TMX5 with the ER marker CNX and with the trans-Golgi marker Giantin. **E** Same as **D** for TMX5$_{C220A}$. **F** Same as **D** for TMX5$_{C114A}$. **G** Same as **D** for TMX5$_{C124A}$. **H** Same as **D** for TMX5$_{C177A}$. **I** Same as **D** for TMX5$_{C210A}$.

5

TMX5 is a natural trapping protein that engages endogenous clients via cysteine 220

We previously assessed the client specificity of the TMX family members *in cellula* (Kucinska *et al.*, 2023; Pisoni *et al.*, 2015). To this end, we generated the clients-trapping mutant forms of TMX1 (Pisoni et al., 2015), TMX3 and TMX4 (Kucinska et al., 2023) by mutating the C-terminal cysteine of the CXXC active site motif to alanine to substantially delay release of the endogenous clients from the oxidoreductases (Fujimoto *et al*, 2019). This operation was unnecessary for TMX5 that has an unconventional CRFS active site that defines TMX5 as a natural trapping protein (Yang et al., 2016). TMX clients were identified upon co-immunoprecipitation and mass spectrometry (Kucinska *et al.*, 2023; Pisoni *et al.*, 2015). For TMX5, a V5-tagged version of the protein was expressed in HEK293 cells. After immunoisolation of TMX5 from cell lysates with anti-V5 antibodies, the immunocomplexes were separated in non-reducing (**Fig. 3A**, NRed) and reducing SDS polyacrylamide gels (**Fig. 3A**, Red), which were subsequently silver stained. Disulfide-bonded complexes between endogenous polypeptides and TMX5 are shown in the gel (**Fig. 3A**, NRed, red rectangle) and their identity established by mass spectrometry is listed in **Fig. 3B** (red column). Upon reduction, the disulfide-bonded complexes are disassembled and disappear from this region of the gel (**Figs. 3A**, Red, blue rectangles). Consistently, the TMX5 clients are identified by their disappearance from MS detection when this region of the reducing gel is probed (**Fig. 3B**, blue column). Among the cellular proteins that form mixed disulfides with TMX5, it is worth mentioning the few members of the PDI superfamily (PDI (P4HB), ERp44, ERp57 (PDIA3)), few secretory proteins, and a large spectrum of single and multipass proteins that reside in the membrane of secretory organelles, with preponderance of Golgi-resident polypeptides (**Fig. 3B**). Notably, the endogenous proteins engaging TMX5 are clearly distinct for the endogenous clients of TMX1 (Pisoni et al., 2015), TMX3 and TMX4 (Kucinska et al., 2023). This confirms the exquisite selectivity of individual members of the PDI superfamily, which results from their distinct substrate interaction domains, different co-factors, and different sub-compartmental distribution (Kanemura *et al*, 2020).

As expected, the replacement of the active site cysteine 220 with an alanine residue substantially hampers the involvement of TMX5 in mixed disulfides (**Fig. 3C**, compare the region shown with *a* in lane 2 *vs.* lane 3). However, we noticed that some covalent interactions were not prevented by this mutation (**Fig. 3C**, shown with *b* in lanes 2 and 3). This shows that select endogenous proteins engage TMX5 by forming mixed disulfides with non-catalytic cysteine residues.
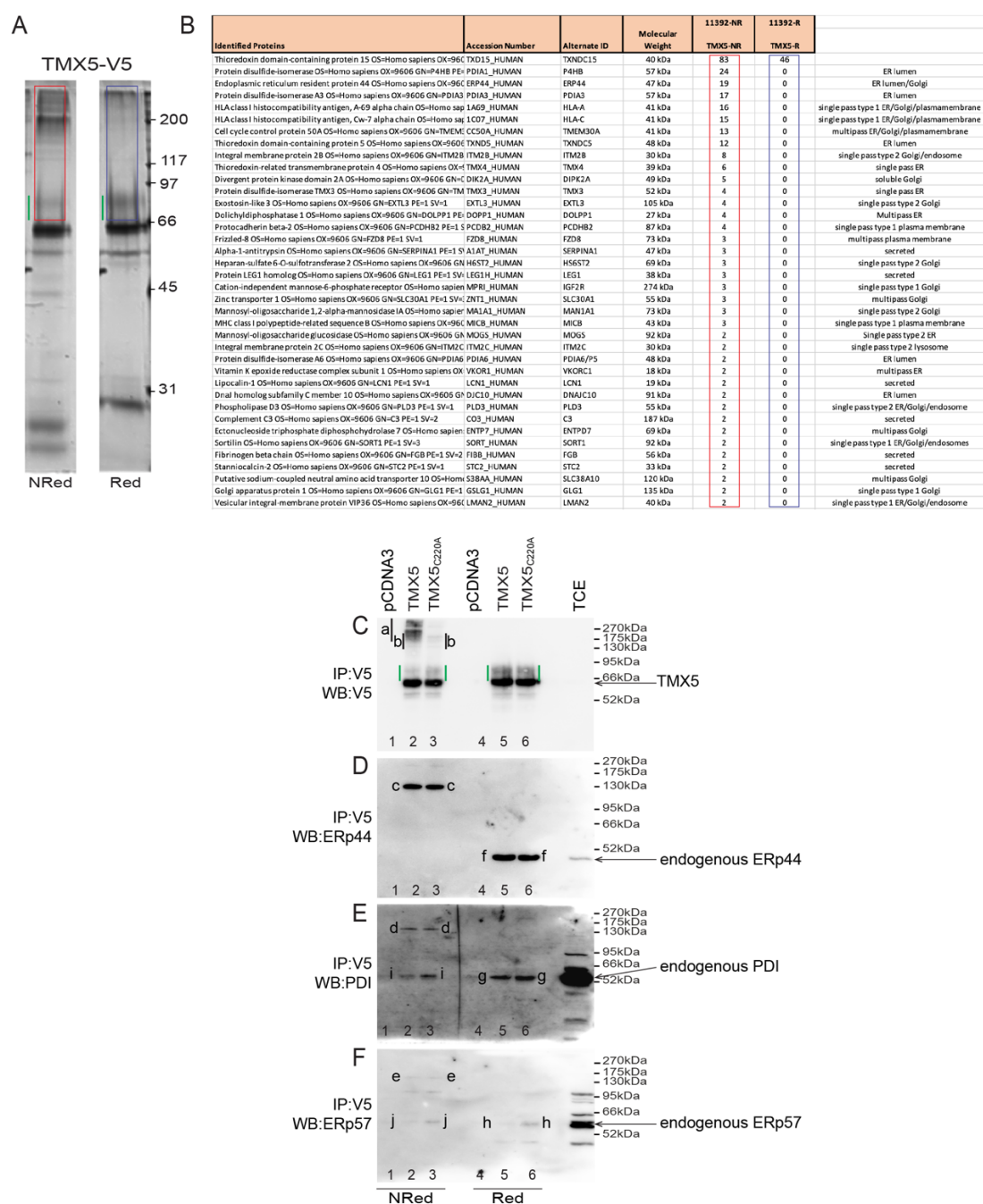
A

TMX5-V5

NRed   Red

B

Identified Proteins	Accession Number	Alternate ID	Molecular Weight	11392-NR TMX5-NR	11392-R TMX5-R	
Thioredoxin domain-containing protein 15 OS=Homo sapiens OX=960	TXD15_HUMAN	TXNDC15	40 kDa	83	46	
Protein disulfide-isomerase OS=Homo sapiens OX=9606 GN=P4HB PE=	PDIA1_HUMAN	P4HB	57 kDa	24	0	ER lumen
Endoplasmic reticulum resident protein 44 OS=Homo sapiens OX=960	ERP44_HUMAN	ERP44	47 kDa	19	0	ER lumen/Golgi
Protein disulfide-isomerase A3 OS=Homo sapiens OX=9606 GN=PDIA3	PDIA3_HUMAN	PDIA3	57 kDa	17	0	ER lumen
HLA class I histocompatibility antigen, A-69 alpha chain OS=Homo sap	1A69_HUMAN	HLA-A	41 kDa	16	0	single pass type 1 ER/Golgi/plasmamembrane
HLA class I histocompatibility antigen, Cw-7 alpha chain OS=Homo sap	1C07_HUMAN	HLA-C	41 kDa	15	0	single pass type 1 ER/Golgi/plasmamembrane
Cell cycle control protein 50A OS=Homo sapiens OX=9606 GN=TMEM3	CC50A_HUMAN	TMEM30A	41 kDa	13	0	multipass ER/Golgi/plasmamembrane
Thioredoxin domain-containing protein 5 OS=Homo sapiens OX=960	TXNDC5_HUMAN	TXNDC5	48 kDa	12	0	ER lumen
Integral membrane protein 2B OS=Homo sapiens OX=9606 GN=ITM2B	ITM2B_HUMAN	ITM2B	30 kDa	8	0	single pass type 2 Golgi/endosome
Thioredoxin-related transmembrane protein 4 OS=Homo sapiens OX=	TMX4_HUMAN	TMX4	39 kDa	6	0	single pass ER
Divergent protein kinase domain 2A OS=Homo sapiens OX=9606 GN=C	DIPK2A_HUMAN	DIPK2A	49 kDa	5	0	soluble Golgi
Protein disulfide-isomerase TMX3 OS=Homo sapiens OX=9606 GN=TM	TMX3_HUMAN	TMX3	52 kDa	4	0	single pass ER
Exostosin-like 3 OS=Homo sapiens OX=9606 GN=EXTL3 PE=1 SV=1	EXTL3_HUMAN	EXTL3	105 kDa	4	0	single pass type 2 Golgi
Dolichyldiphosphatase 1 OS=Homo sapiens OX=9606 GN=DOLPP1 PE=	DOPP1_HUMAN	DOLPP1	27 kDa	4	0	Multipass ER
Protocadherin beta-2 OS=Homo sapiens OX=9606 GN=PCDHB2 PE=1 S	PCDB2_HUMAN	PCDHB2	87 kDa	4	0	single pass type 1 plasma membrane
Frizzled-8 OS=Homo sapiens OX=9606 GN=FZD8 PE=1 SV=1	FZD8_HUMAN	FZD8	73 kDa	3	0	multipass plasma membrane
Alpha-1-antitrypsin OS=Homo sapiens OX=9606 GN=SERPINA1 PE=1 S	A1AT_HUMAN	SERPINA1	47 kDa	3	0	secreted
Heparan-sulfate 6-O-sulfotransferase 2 OS=Homo sapiens OX=9606 GN	HS6ST2_HUMAN	HS6ST2	69 kDa	3	0	single pass type 2 Golgi
Protein LEG1 homolog OS=Homo sapiens OX=9606 GN=LEG1 PE=1 SV=	LEG1H_HUMAN	LEG1	38 kDa	3	0	secreted
Cation-independent mannose-6-phosphate receptor OS=Homo sapien	MPRI_HUMAN	IGF2R	274 kDa	3	0	single pass type 1 Golgi
Zinc transporter 1 OS=Homo sapiens OX=9606 GN=SLC30A1 PE=1 SV=	ZNT1_HUMAN	SLC30A1	55 kDa	3	0	multipass Golgi
Mannosyl-oligosaccharide 1,2-alpha-mannosidase IA OS=Homo sapien	MA1A1_HUMAN	MAN1A1	73 kDa	3	0	single pass type 2 Golgi
MHC class I polypeptide-related sequence B OS=Homo sapiens OX=96	MICB_HUMAN	MICB	43 kDa	3	0	single pass type 1 plasma membrane
Mannosyl-oligosaccharide glucosidase OS=Homo sapiens OX=9606 GN	MOGS_HUMAN	MOGS	92 kDa	2	0	Single pass type 2 ER
Integral membrane protein 2C OS=Homo sapiens OX=9606 GN=ITM2C	ITM2C_HUMAN	ITM2C	30 kDa	2	0	single pass type 2 lysosome
Protein disulfide-isomerase A6 OS=Homo sapiens OX=9606 GN=PDIA6	PDIA6/P5	PDIA6/P5	48 kDa	2	0	ER lumen
Vitamin K epoxide reductase complex subunit 1 OS=Homo sapiens OX	VKOR1_HUMAN	VKORC1	18 kDa	2	0	multipass ER
Lipocalin-1 OS=Homo sapiens OX=9606 GN=LCN1 PE=1 SV=1	LCN1_HUMAN	LCN1	19 kDa	2	0	secreted
DnaJ homolog subfamily C member 10 OS=Homo sapiens OX=9606 GN	DJC10_HUMAN	DNAJC10	91 kDa	2	0	ER lumen
Phospholipase D3 OS=Homo sapiens OX=9606 GN=PLD3 PE=1 SV=1	PLD3_HUMAN	PLD3	55 kDa	2	0	single pass type 2 ER/Golgi/endosome
Complement C3 OS=Homo sapiens OX=9606 GN=C3 PE=1 SV=2	CO3_HUMAN	C3	187 kDa	2	0	secreted
Ectonucleoside triphosphate diphosphohydrolase 7 OS=Homo sapien	ENTP7_HUMAN	ENTPD7	69 kDa	2	0	multipass Golgi
Sortilin OS=Homo sapiens OX=9606 GN=SORT1 PE=1 SV=3	SORT_HUMAN	SORT1	92 kDa	2	0	single pass type 1 ER/Golgi/endosomes
Fibrinogen beta chain OS=Homo sapiens OX=9606 GN=FGB PE=1 SV=2	FIBB_HUMAN	FGB	56 kDa	2	0	secreted
Stanniocalcin-2 OS=Homo sapiens OX=9606 GN=STC2 PE=1 SV=1	STC2_HUMAN	STC2	33 kDa	2	0	secreted
Putative sodium-coupled neutral amino acid transporter 10 OS=Hom	S38AA_HUMAN	SLC38A10	120 kDa	2	0	multipass Golgi
Golgi apparatus protein 1 OS=Homo sapiens OX=9606 GN=GLG1 PE=1	GSLG1_HUMAN	GLG1	135 kDa	2	0	single pass type 1 Golgi
Vesicular integral-membrane protein VIP36 OS=Homo sapiens OX=960	LMAN2_HUMAN	LMAN2	40 kDa	2	0	single pass type 1 ER/Golgi/endosome

pCDNA3 TMX5 TMX5$_{C220A}$ pCDNA3 TMX5 TMX5$_{C220A}$ TCE

C

IP:V5
WB:V5

— 270kDa
— 175kDa
— 130kDa
— 95kDa
— 66kDa TMX5
— 52kDa

1 2 3   4 5 6

D

IP:V5
WB:ERp44

— 270kDa
— 175kDa
— 130kDa
— 95kDa
— 66kDa
— 52kDa ← endogenous ERp44

1 2 3   4 5 6

E

IP:V5
WB:PDI

— 270kDa
— 175kDa
— 130kDa
— 95kDa
— 66kDa ← endogenous PDI
— 52kDa

1 2 3   4 5 6

F

IP:V5
WB:ERp57

— 270kDa
— 175kDa
— 130kDa
— 95kDa
— 66kDa ← endogenous ERp57
— 52kDa

1 2 3   4 5 6

NRed   Red

Figure 3. Endogenous interactors of TMX5. A V5-tagged TMX5 has been immunoisolated from HEK293 cell lysates. Part of the immunocomplexes were separated in non-reducing/reducing gel and stained with Silver. The endogenous proteins engaged in mixed disulfides with TMX5 (red rectangle) have been identified by LC/MS analyses after trypsin digestion in gel (two independent experiments). **B** Endogenous polypeptides engaged by TMX5 in mixed disulfides are shown in the red rectangle. **C** The engagement of TMX5 clients in mixed disulfides (lane 2) is substantially inhibited upon replacement of the active site Cys$_{220}$ with alanine (lane 3). *a* shows TMX clients engaged by the active site Cys$_{220}$; *b* shows interaction partners, whose covalent association persists upon mutation of the active site cysteine; green lines show complex glycosylated TMX5. **D** *c* shows the endogenous ERp44 component of TMX5 complexes immunoisolated with anti-V5 antibodies. Upon reduction of the sample, the disulfide bonded complexes are disassembled and the ERp44 component is shown with *f*. ERp44 is engaged in mixed disulfides both with TMX5 (lane 2) and with TMX5$_{C220A}$ (lane 3). **E** Same as **D** for PDI. Note that PDI also associates non-covalently with TMX5 and TMX5$_{C220A}$ (shown with i). **F** Same as **D** for ERp57. Note that ERp57 also associates non-covalently with TMX5 and TMX5$_{C220A}$ (shown with j).

7

ERp44 form mixed disulfides engaging the non-catalytic cysteines of TMX5

Analyses of the polypeptides that maintained the covalent association with TMX5$_{C220A}$ (**Fig. 3C**, lane 3, shown with *b*) reveal several members of the PDI superfamily. In fact, both the immunoisolation of TMX5 and of the catalytically inactive TMX5$_{C220A}$ results in the capture of disulfide bonded endogenous ERp44 (**Fig. 3D**, lanes 2-3, *c*), of disulfide-bonded endogenous PDI (**Fig. 3E**, lanes 2-3, *d*), of disulfide bonded endogenous ERp57 (**Fig. 3F**, lanes 2-3, *e*). These covalent complexes disappear upon reduction (**Figs. 3D-3F**, lanes 5-6) and the signals collapse into the monomeric forms of ERp44 (**Fig. 3D**, *f*), PDI (**Fig. 3E**, *g*) or ERp57 (**Fig. 3F**, *h*). PDI and ERp57 also associate non-covalently with TMX5 as shown by their monomeric forms that co-precipitate both with TMX5 and with the catalytically inactive TMX5$_{C220A}$ (shown with *i* and *j*, respectively in **Figs. 3E, 3F**, lanes 2-3). These data reveal that PDI, ERp57 and ERp44 are not clients of TMX5. Rather, they could play a role in ruling the biological activity of TMX5 by acting as co-factors. PDI and ERp57 oxidoreductases could regulate the release of clients from TMX5. In fact, the N-terminal cysteine of the TMX5 active site can nucleophilically attack a free thiol group in protein substrates, but the interactions can be resolved only by the intervention of an external cysteine provided by glutathione, or by another PDI (Yang *et al.*, 2016). More interesting in the context of our study is the covalent association of TMX5 with ERp44, an unconventional member of the PDI superfamily previously reported to regulate the positioning in the secretory line of proteins lacking the ER retrieval sequence (Otsu *et al*, 2006; Tempio & Anelli, 2020), a feature that TMX5 shares with a number of polypeptides acting in early compartments of the secretory line.

The covalent association of ERp44 with TMX5 relies on ERp44's cysteine residue 29

Notably, complex glycosylation is not observed for TMX3 and TMX4 that, in contrast to TMX5, possess C-terminal KKXX retention sequences that efficiently retains them in the ER or in the contiguous nuclear envelope membrane (Guerra *et al.*, 2018; Guerra & Molinari, 2020; Kucinska *et al.*, 2023; Pisoni *et al.*, 2015). In this context, the finding that endogenous ERp44 is a major interacting partner of TMX5 (**Figs. 3B, 3D**) is relevant. In fact, ERp44 cycles between ER and Golgi to ensure the retention of key factors designed to act in the ER but devoid of suitable localization motifs including Ero1α, Ero1β, Prx4, ERAP1, SUMF1 (Fraldi *et al*, 2008). The ER retention function of ERp44 is exerted by interacting with clients via the catalytic site cysteine residue at position 29 (Tempio & Anelli, 2020). To

8

verify whether the active site Cys_{29} of ERp44 is involved in the association with TMX5, HA-tagged ERp44 or $ERp44_{C29S}$ were co-expressed in HEK293 cells with V5-tagged TMX5. Complexes were immunoisolated from detergent lysates with anti-V5 antibodies and separated under non reducing or reducing conditions to verify the presence of HA-tagged ERp44 and $ERp44_{C29S}$ in the immunocomplexes by WB (**Figs. 4A, 4B**, respectively). Analyses of the WB confirm that ERp44 engages TMX5 in mixed disulfides (shown with *a*, lane 2, **Fig. 4A**), whereas $ERp44_{C29S}$ does so with much reduced magnitude (lane 3).
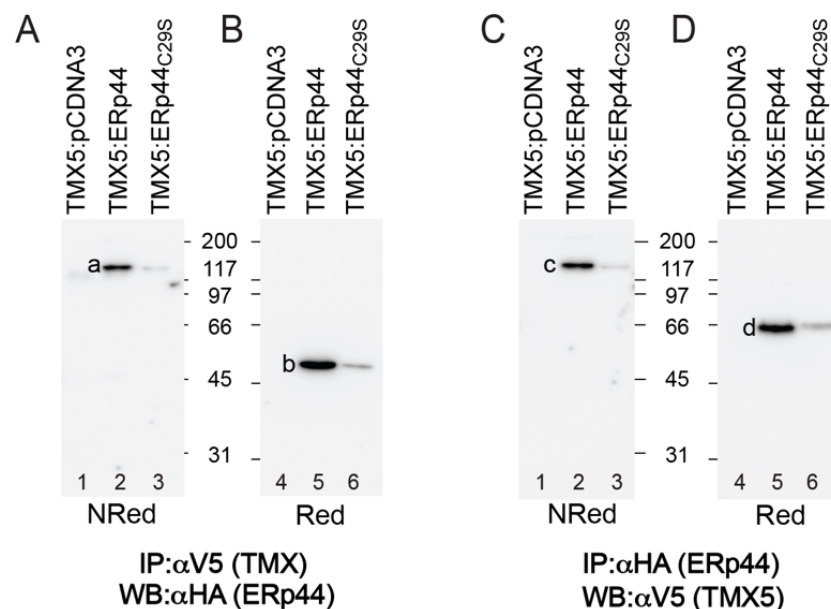
Figure 4. TMX5 engages ERp44 in mixed disulfides via its catalytic Cys_{29}. A Formation of mixed disulfides between TMX5 and ERp44 (lane 2) or $ERp44_{C29S}$ (lane 3). Mixed disulfides are immunoisolated with anti-V5 antibodies, are separated in nonreducing SDS-PAGE. The ERp44 component (indicated with *a*) is seen by WB with an anti HA antibody. **B** Same as **A** , but the mixed disulfides are disassembled by running the gel under reducing conditions. *b* shows ERp44. **C** Same as **A** where the mixed disulfides have been immunoisolated from detergent extract with an anti-HA antibody and the TMX5 component is revealed in WB with an anti-V5 antibody (indicated with *c*). **D** Same as **B** for the TMX5 (indicated with *d*).

Disassembly of the complexes under reducing conditions reveals the ERp44 component of the mixed disulfides (shown with *b*, lane 5, **Fig 4B**). The composition of the complexes was confirmed by their immunoisolation with an anti-HA antibody to capture the ERp44 component, and detection of the TMX5 component in WB with an anti-V5 antibody (**Figs. 4C, 4D**, lanes 2 and 5). Notably, the TMX5 that co-precipitates with ERp44 (**Fig. 4D**, lane 5, shown with d) lacks the slow migrating, complex glycosylated polypeptide fraction that cycles in the Golgi compartment shown with green lines in **Figs. 2A, 2B, 3A, 3C**. Thus, ERp44 associates covalently via the active site Cys_{29} with the population of TMX5 located in the ER and prevents its delivery to the Golgi compartment.

The covalent association of ERp44 with TMX5 relies on TMX5's cysteine residues 114 and 124

Mutation of the catalytic site Cys_{220} of TMX5 does not inhibit the covalent association of endogenous ERp44 (**Fig. 3D**). To establish the TMX5 cysteine residue(s) involved in the mixed disulfide with ERp44, HA-tagged ERp44 was co-expressed with individual V5-tagged cysteine mutants of TMX5 in HEK293 cells.
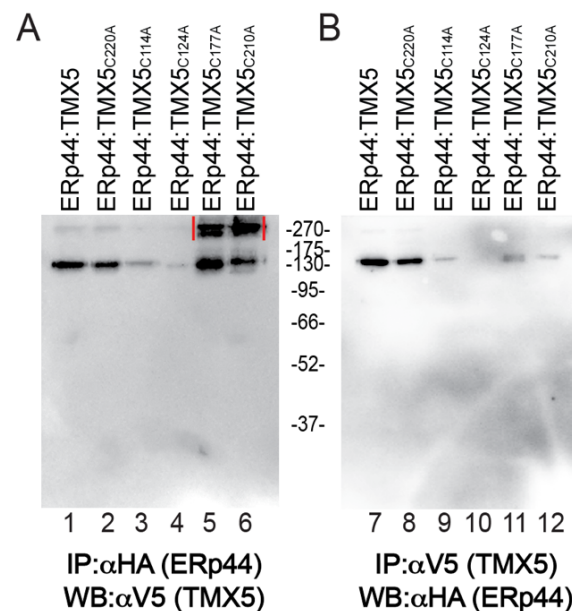

Figure 5. ERp44 engages Cys_{114} and/or Cys_{124} of TMX5 in mixed disulfides. A Co-precipitation of cysteine mutants of TMX5 with ERp44. The mixed disulfides are separated in a non-reducing gel. Here the TMX5 component of the ERp44-S-S-TMX5 complex is shown. **B** Co-precipitation of ERp44 with TMX5. The ERp44 component of the ERp44-S-S-TMX5 complex is shown in the non-reducing gel.

The formation of covalent complexes between ERp44 and TMX5 variants was tested upon immunoisolation of the complexes with anti-HA antibodies, separation of the immunocomplexes in non-reducing/reducing WB and detection of the TMX5 interacting partner with anti-V5 antibodies. As shown in **Fig. 3D**, ERp44 engages in mixed disulfides with TMX5 (**Fig. 5**, lane 1) and $TMX5_{C220A}$ (**Fig. 5**, lane 2). The mutation of Cys_{114} and of Cys_{124} to alanine residues prevents covalent engagement of the TMX5 protein by the active site cysteine of ERp44 (lanes 3, 4). Mutations of Cys_{177} (lane 5) and of Cys_{210} (lane 6) allows the covalent engagement of TMX5 with formation of aberrant complexes possibly resulting from TMX5 misfolding/instability due to deletion of the structural disulfide that binds these two cysteine residues (red lines, lanes 5, 6). Thus, the active site Cys_{29} of ERp44 engages Cys_{114} and Cys_{124} of TMX5 in mixed disulfides.

10

The association with ERp44 retains TMX5 in the ER and reduces engagement of endogenous clients

The co-expression of active ERp44 substantially reduces the fraction of TMX5 engaged with endogenous clients in mixed disulfides (compare **Fig. 6A**, lanes 1 *vs.* 2, shown with *a*). The co-expression of the ERp44$_{C29S}$ mutant that does not engage TMX5 in covalent complexes (**Fig. 4**), does not affect the formation of mixed disulfides between TMX5 and its clients (**Fig. 6A**, lane 3).
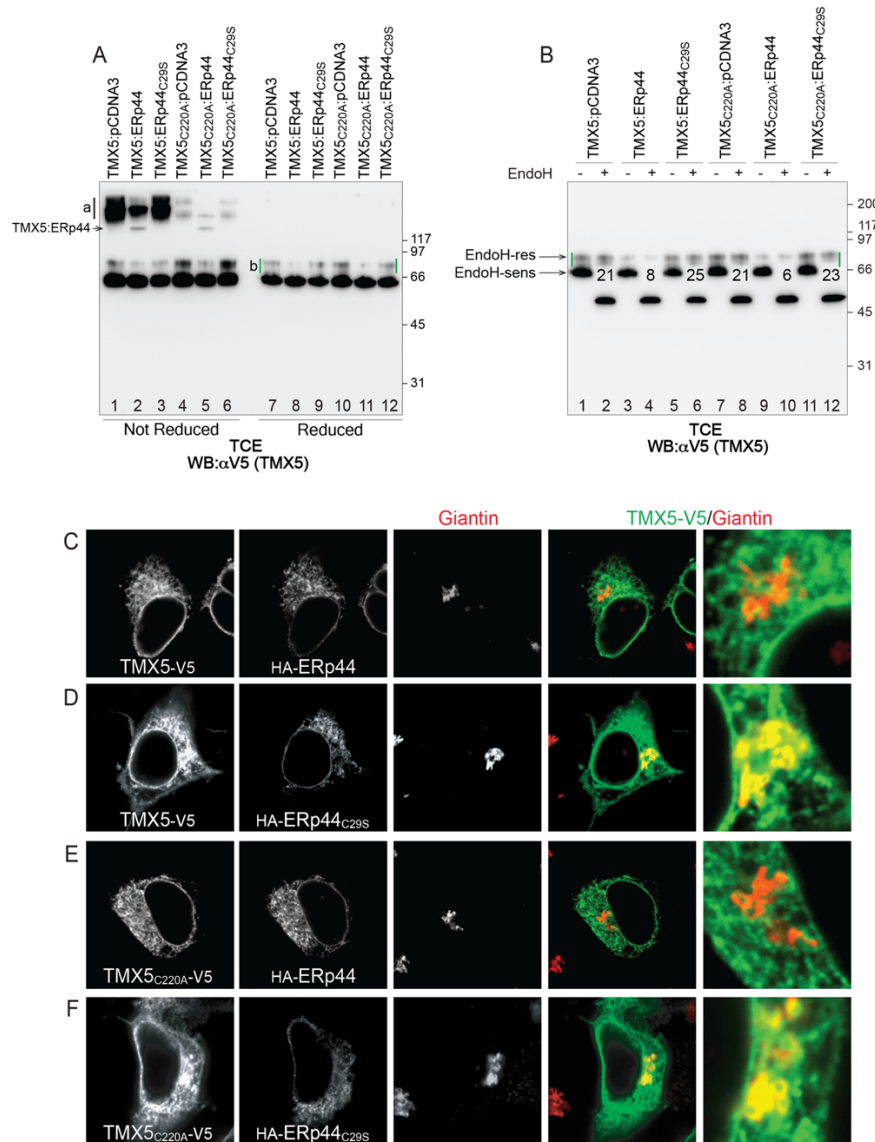

Figure 6. The association with ERp44 retains TMX5 in the ER and reduces engagement of endogenous clients. A Western blot analysis of post nuclear fractions of HEK293 cells co-transfected with V5-tagged TMX5 and HA-tagged ERp44 or ERp44$_{C29S}$. The TMX component of the complexes is revealed with anti-V5 antibody in non-reducing and reducing conditions (lanes 1-6 and 7-12, respectively). Mixed disulfides between TMX5 and endogenous clients are shown with the black line *a*. TMX5:ERp44 mixed disulfides are shown in lanes 2 and 5. The complex glycosylated, Golgi form of TMX5 is shown with the green lines *b*. **B** EndoH assay of the same samples. The EndoH-resistant, Golgi forms of TMX5 are shown with green lines. The % of EndoH-resistant TMX5's form is given for this experiment. **C** Lack of co-localization of TMX5 with the Golgi marker Giantin upon co-expression of active ERp44. **D** Co-localization of a fraction of TMX5 with Giantin upon co-expression of inactive ERp44$_{C29S}$. **E** Same as **C** for inactive TMX5$_{C220A}$. **F** Same as **D** for inactive TMX5$_{C220A}$ showing lack of co-localization with Giantin upon co-expression of ERp44$_{C29S}$.

11

Analyses of the electrophoretic mobility of TMX5 (**Fig. 6A**, lanes 7-12, green lines) and the EndoH assay (**Fig. 6B**) also reveal that the association with ERp44 retains TMX5 in the ER as shown by the substantial reduction in TMX5 complex glycosylation from about 20% EndoH-resistant fraction in mock-transfected cells (**Figs. 2B, 6B**, lanes 1, 2) and in cells expressing ERp44$_{C29S}$ (**Fig. 6B**, lanes 5, 6) to less than 10% (**Fig. 6B**, lanes 3, 4). Replacement of the active site TMX5 cysteine 220 with alanine, abolishes the engagement of clients in mixed disulfides (**Figs. 3C, 6A**, lanes 4-6). This mutation does not affect the fraction of TMX5 that acquires EndoH-resistant N-glycans as symptom of ER to Golgi trafficking (**Figs. 6B**, lane 7, 8), does not prevent engagement of ERp44 (**Fig. 3D**), nor the capacity of ERp44 to inhibit release of TMX5 from the ER (**Figs. 6B**, lanes 9-12). The role of ERp44 in determining the intracellular localization of TMX5 has been confirmed by CLSM showing that TMX5 and TMX5$_{C220A}$ are excluded from the Golgi compartment when co-expressed with active ERp44 (**Figs. 6C, 6E**), but traffic to the Golgi compartment when co-expressed with the active site mutant form ERp44$_{C29S}$ (**Figs. 6D, 6F**).

All in all, our study offers a preliminary set of information on a neglected member of the PDI family by showing that TMX5 engages a subset of cellular proteins in mixed disulfide via the active site cysteine 220. TMX5 clients are clearly distinct from the clients of TMX1 (Pisoni et al., 2015), TMX3 and TMX4 (Kucinska et al., 2023) confirms the selectivity of individual members of the PDI superfamily, which results from their distinct substrate interaction domains, different co-factors, and different sub-compartmental distribution (Kanemura *et al.*, 2020). Unfortunately, our attempts to silence the expression of TMX5 failed, and we were therefore unable to evaluate the consequences of lack of TMX5 on the client's fate. Our results allow to add TMX5 to the limited group of proteins including Ero1α, Ero1β, Prx4, ERAP1, SUMF1 that lack the ER retrieval sequence and rely on ERp44 engagement to control their sub-cellular localization. Notably, in contrast to the other ERp44 clients, TMX5 is tethered at the ER membrane. Why these proteins that exert most of their known activities in the ER do not rely on conventional C-terminal retention/retrieval sequences to be retained in the compartment is a matter of discussion, but it is likely that under specific circumstances, they are called to exerts action in the Golgi compartment, at the cell surface, or extracellularly (Tempio & Anelli, 2020).

Materials and Methods

Cell Culture, Transient Transfection

Human Embryonic Kidney 293 (HEK293) and Mouse Embryonic Fibroblasts (MEF) cell lines were cultured at 37°C and 5% CO2 in Dulbecco's Modified Eagle Medium (DMEM) with high glucose (GlutaMAX™, Gibco) supplemented with 10% Fetal bovine serum (FBS, Gibco). Transient transfections were carried out using JetPrime (Polypus) in DMEM 10% FBS supplemented with non-essential amino acids (NEAA, Gibco) following the manufacturer's protocol. Experiments were performed 17h after transfection.

Antibodies and expression plasmids

S1 Table: details of antibodies used. Plasmids encoding for TMX5-V5 WT and cysteine mutants were synthesized by Genscript in pUC57 and subcloned in pcDNA3.1(-) through restriction digestion of BamHI and HindIII (NEB) sites flanking the target sequence. Ligation was carried out using T4 DNA ligase (NEB) at a 3:1 insert to vector ratio, following the manufacturer's protocol. Plasmids were subsequently amplified and isolated from JM109 bacteria (Promega) using the GenElute™ HP plasmid MidiPrep kit (Sigma). Plasmids for expression of ERp44wt and C29S mutant were a kind gift of Roberto Sitia.

Cell lysis, Immunoprecipitation (IP), Western Blot (WB) and EndoH treatment

HEK293 cells were washed with ice-cold 1xPBS containing 20 mM N-ethylmaleimide (NEM), then lysed with RIPA buffer containing 20 mM NEM and protease inhibitors (1 mM phenylmethylsulfonyl fluoride (PMSF), 16.5 mM Chymostatin, 23.4 mM Leupeptin, 16.6 mM Antipain, 14.6 mM Pepstatin) for 20 min on ice. Lysates were subjected to centrifugation for 10 min at 4°C, 10,600 g to extract the post-nuclear supernatant (PNS). For immunoprecipitation PNS were incubated with Anti-V5 Agarose Affinity Gel conjugated beads or with Protein-A beads (Sigma, 1:10 w/v swollen in PBS) and anti-HA antibody for 2 h at 4°C. Samples were than washed with 1% Triton in HBS 1x pH 7.4 and then dried. Dried beads were resuspended in sample buffer and boiled at 95°C for 5 min. After boiling, samples without (Non reducing) or with 100mM DTT (Roche)(reducing) were subjected to SDS-PAGE. For detection of proteins by Western Blot (WB) protein bands (IP or TCE) were transferred from polyacrylamide gel to a PVDF membrane using a TransBlot Turbo device (BioRad). PVDF membrane was blocked for 10 min with 8% blocking milk in Tris-buffered saline, 0.1% Tween 20 (v/v) (TBS-T) and incubated with primary antibodies (Table **S1**) with shaking. After primary antibody washout with TBS-T, membranes were incubated with HRP-conjugated secondary antibody or with HRP-conjugated protein A (Table **S1**) for 45 min at RT while shaking. Protein bands were detected on a Fusion FX7 chemiluminescence detection system (Vilber) using WesternBright™ Quantum or WesternBright ECL HRP Substrate (Witec AG) following the manufacturer's protocol. Protein bands were quantified with FIJI/ImageJ software. For EndoH (NEB) treatment proteins from immunoprecipitated samples or from TCE were split into two aliquots and incubated in the presence or absence of 5mU of EndoH for 3 h at 37 °C according to the manufacturer's protocol. Samples were then analyzed by SDS-PAGE.

Mass spectrometry

HEK cells, transfected with an empty vector or transfected with V5-tagged TMX5 were rinsed with PBS and 20 mM NEM. Cells were lysed with RIPA buffer supplemented with 20 mM NEM and protease inhibitors for 20 min on ice. PNS Immunoisolated with anti V5 Agarose beads were washed three times with 1% Triton in HBS 1x pH 7.4 and then dried. Mass spectrometry analysis was performed at the Protein Analysis Facility, University of Lausanne, Lausanne, Switzerland.

Confocal laser scanning microscopy (CLSM)

HEK cells were seeded on poly-L coated (Sigma) glass coverslips (VWR) and transiently transfected as indicated using JetPrime (Polypus) in DMEM 10% FBS supplemented with NEAA (Gibco). Seventeen hours after transfection, cells were fixed at RT for 20 min in 3.7% formaldehyde (FA, v/v) in PBS. Coverslips were incubated

for 20 min in permeabilization solution (PS, 10 mM HEPES, 15 mM glycine, 10% goat serum (v/v), 0.05% saponin (w/v)). Following permeabilization, primary antibodies (Table S1) diluted 1:100 in PS were applied for 2 h, washed three times in PS, and then incubated with Alexa Fluor-conjugated secondary antibodies diluted 1:300 in PS for 45 min. Cells were washed three times with PS and once with deionized water and mounted on a drop of Vectashield (Vector Laboratories) supplemented with 40,6-diamidino-2-phenylindole (DAPI). Coverslips were imaged using a Leica TCS SP5, microscope equipped with Leica HCX PL APO lambda blue 63.0 × 1.40 oil objective. Leica LAS X software was used for image acquisition, with excitation provided by 488-, 561-, and 633-nm lasers and fluorescence light was collected within the ranges of 504-587 nm (AlexaFluor488), 557-663 nm (TMR) and 658-750 nm (AlexaFluor646), respectively with pinhole 1 AU. Image post-processing was performed with Adobe Photoshop.

S1 Table. Details of antibodies used.

Antibody	Manufacturer	Catalog number	Dilution or Concentration
Mouse anti-V5	Thermo Fisher Scientific	R96025	1:5000 (IB); 1:100 (CLSM)
Rabbit anti-HA	Sigma	H6908	1:3000 (IB); 1:100 (CLSM)
Anti-V5 Agarose Affinity Gel antibody	Sigma	A7345	
Rabbit anti-CNX	Kind gift from A. Helenius	Not applicable	1:3000 (IB)
Mouse anti-GAPDH	Merck	MAB374	1:30000 (IB)
Rabbit anti-ERp44	Kind gift from R. Sitia		1:1000 (IB)
Rabbit anti-PDI	Stessgen	SPA890	1:1000 (IB)
Rabbit anti-ERp57	Kind gift from G. Hämmerling		1:1000 (IB)
Rabbit anti-Giantin	Biolegend	920342	1:100 (CLSM)
Protein A HRP-conjugated	Invitrogen	101023	1:20000 (IB)
Goat anti-mouse HRP-conjugated	Southern Biotech	1031-05	1:20000 (IB)

Anelli T, Alessio M, Mezghrani A, Simmen T, Talamo F, Bachi A, Sitia R (2002) ERp44, a novel endoplasmic reticulum folding assistant of the thioredoxin family. *Embo J* 21: 835-844

Chen J, Yap MC, Bassot A, Pascual DM, Makio T, Zimmermann J, Mast H, Bhat R, Fleury SG, Fan Y *et al* (2024) The ER Thioredoxin-Related Transmembrane Protein TMX2 Controls Redox-Mediated Tethering of ER-Mitochondria Contacts. *bioRxiv*

Deng T, Xie Y (2024) Novel homozygous mutations in TXNDC15 causing Meckel syndrome. *Mol Genet Genomic Med* 12: e2343

Fraldi A, Zito E, Annunziata F, Lombardi A, Cozzolino M, Monti M, Spampanato C, Ballabio A, Pucci P, Sitia R *et al* (2008) Multistep, sequential control of the trafficking and function of the multiple sulfatase deficiency gene product, SUMF1 by PDI, ERGIC-53 and ERp44. *Hum Mol Genet* 17: 2610-2621

Fujimoto T, Inaba K, Kadokura H (2019) Methods to identify the substrates of thiol-disulfide oxidoreductases. *Protein Sci* 28: 30-40

Guerra C, Brambilla Pisoni G, Solda T, Molinari M (2018) The reductase TMX1 contributes to ERAD by preferentially acting on membrane-associated folding-defective polypeptides. *Biochem Biophys Res Commun* 503: 938-943

Guerra C, Molinari M (2020) Thioredoxin-Related Transmembrane Proteins: TMX1 and Little Brothers TMX2, TMX3, TMX4 and TMX5. *Cells* 9: 1-11

Hartill V, Szymanska K, Sharif SM, Wheway G, Johnson CA (2017) Meckel-Gruber Syndrome: An Update on Diagnosis, Clinical Management, and Research Advances. *Frontiers in Pediatrics* 5: 1-9

Hatahet F, Ruddock LW (2009) Modulating proteostasis: peptidomimetic inhibitors and activators of protein folding. *Curr Pharm Des* 15: 2488-2507

Haugstetter J, Blicher T, Ellgaard L (2005) Identification and characterization of a novel thioredoxin-related transmembrane protein of the endoplasmic reticulum. *J Biol Chem* 280: 8371-8380

Haugstetter J, Maurer MA, Blicher T, Pagac M, Wider G, Ellgaard L (2007) Structure-function analysis of the endoplasmic reticulum oxidoreductase TMX3 reveals interdomain stabilization of the N-terminal redox-active domain. *J Biol Chem* 282: 33859-33867

Herrera-Cruz MS, Yap MC, Tahbaz N, Phillips K, Thomas L, Thomas G, Simmen T (2021) Rab32 uses its effector reticulon 3L to trigger autophagic degradation of mitochondria-associated membrane (MAM) proteins. *Biol Direct* 16: 1-16

Kanemura S, Matsusaki M, Inaba K, Okumura M (2020) PDI Family Members as Guides for Client Folding and Assembly. *Int J Mol Sci* 21: 1-20

Kucinska MK, Fedry J, Galli C, Morone D, Raimondi A, Solda T, Forster F, Molinari M (2023) TMX4-driven LINC complex disassembly and asymmetric autophagy of the nuclear envelope upon acute ER stress. *Nat Commun* 14: 1-20

Kucinska MK, Molinari M (2024) Control of nuclear envelope dynamics during acute ER stress by LINC complexes disassembly and selective, asymmetric autophagy of the outer nuclear membrane. *Autophagy* 20: 1-3

Lynes EM, Bui M, Yap MC, Benson MD, Schneider B, Ellgaard L, Berthiaume LG, Simmen T (2012) Palmitoylated TMX and calnexin target to the mitochondria-associated membrane. *The EMBO journal* 31: 457-470

Matsuo Y, Akiyama N, Nakamura H, Yodoi J, Noda M, Kizaka-Kondoh S (2001) Identification of a novel thioredoxin-related transmembrane protein. *The Journal of biological chemistry* 276: 10032-10038

Matsuo Y, Masutani H, Son A, Kizaka-Kondoh S, Yodoi J (2009) Physical and functional interaction of transmembrane thioredoxin-related protein with major histocompatibility complex class I heavy chain: redox-based protein quality control and its potential relevance to immune responses. *Molecular biology of the cell* 20: 4552-4562

Oguro A, Imaoka S (2019) Thioredoxin-related transmembrane protein 2 (TMX2) regulates the Ran protein gradient and importin-beta-dependent nuclear cargo transport. *Sci Rep* 9: 15296

Okumura M, Kadokura H, Inaba K (2015) Structures and functions of protein disulfide isomerase family members involved in proteostasis in the endoplasmic reticulum. *Free Radic Biol Med* 83: 314-322

Otsu M, Bertoli G, Fagioli C, Guerini-Rocco E, Nerini-Molteni S, Ruffato E, Sitia R (2006) Dynamic retention of Ero1alpha and Ero1beta in the endoplasmic reticulum by interactions with PDI and ERp44. *Antioxid Redox Signal* 8: 274-282

Patel C, Saad H, Shenkman M, Lederkremer GZ (2020) Oxidoreductases in Glycoprotein Glycosylation, Folding, and ERAD. *Cells* 9: 1-17

Pisoni GB, Molinari M (2016) Five Questions (with their Answers) on ER-Associated Degradation. *Traffic* 17: 341-350

Pisoni GB, Ruddock LW, Bulleid N, Molinari M (2015) Division of labor among oxidoreductases: TMX1 preferentially acts on transmembrane polypeptides. *Molecular Biology of the Cell* 26: 3390-3400

Quimby BB, Corbett AH (2001) Nuclear transport mechanisms. *Cell Mol Life Sci* 58: 1766-1773

Raturi A, Gutiérrez T, Ortiz-Sandoval C, Ruangkittisakul A, Herrera-Cruz MS, Rockley JP, Gesson K, Ourdev D, Lou PH, Lucchinetti E *et al* (2016) TMX1 determines cancer cell metabolism as a thiol-based modulator of ER mitochondria Ca flux. *Journal of Cell Biology* 214: 433-444

Rothman JE, Urbani LJ, Brands R (1984) Transport of protein between cytoplasmic membranes of fused cells: correspondence to processes reconstituted in a cell-free system. *The Journal of cell biology* 99: 248-259

Sugiura Y, Araki K, Iemura S, Natsume T, Hoseki J, Nagata K (2010) Novel Thioredoxin-related Transmembrane Protein TMX4 Has Reductase Activity. *J Biol Chem* 285: 7135-7142

Tempio T, Anelli T (2020) The pivotal role of ERp44 in patrolling protein secretion. *J Cell Sci* 133: 1-13

Xu H, Pu J, Yang N, Wu Z, Han C, Yao J, Li X (2024) First preimplantation genetic testing case of Meckel syndrome with a novel homozygous TXNDC15 variant in a non-consanguineous Chinese family. *Mol Genet Genomic Med* 12: e2340

Yang K, Li DF, Wang X, Liang J, Sitia R, Wang CC, Wang X (2016) Crystal Structure of the ERp44-Peroxiredoxin 4 Complex Reveals the Molecular Mechanisms of Thiol-Mediated Protein Retention. *Structure* 24: 1755-1765